Journal of Optics

PAPER • OPEN ACCESS

Ultra-fast transient plasmonics using transparent conductive oxides

To cite this article: Marcello Ferrera and Enrico G Carnemolla 2018 *J. Opt.* **20** 024007

View the article online for updates and enhancements.

Ultra-fast transient plasmonics using transparent conductive oxides

Marcello Ferrera and Enrico G Carnemolla

Institute of Photonics and Quantum Sciences, Heriot-Watt University, SUPA, Edinburgh, Scotland, EH14 4AS, United Kingdom

E-mail: m.ferrera@hw.ac.uk

CrossMark

Abstract

During the last decade, plasmonic- and metamaterial-based applications have revolutionized the field of integrated photonics by allowing for deep subwavelength confinement and full control over the effective permittivity and permeability of the optical environment. However, despite the numerous remarkable proofs of principle that have been experimentally demonstrated, few key issues remain preventing a widespread of nanophotonic technologies. Among these fundamental limitations, we remind the large ohmic losses, incompatibility with semiconductor industry standards, and largely reduced dynamic tunability of the optical properties. In this article, in the larger context of the new emerging field of all-dielectric nanophotonics, we present our recent progresses towards the study of large optical nonlinearities in transparent conducting oxides (TCOs) also giving a general overview of the most relevant and recent experimental attainments using TCO-based technology. However, it is important to underline that the present article does not represent a review paper but rather an original work with a broad introduction. Our work lays in a sort of 'hybrid' zone in the middle between high index contrast systems, whose behaviour is well described by applying Mie scattering theory, and standard plasmonic elements where optical modes originate from the electromagnetic coupling with the electronic plasma at the metal-to-dielectric interface. Beside remaining in the context of plasmonic technologies and retaining all the fundamental peculiarities that promoted the success of plasmonics in the first place, our strategy has the additional advantage to allow for large and ultra-fast tunability of the effective complex refractive index by accessing the index-near-zero regime in bulk materials at telecom wavelength.

Keywords: Nanophotonics, plasmonics, alternative materials, nonlinear optics

(Some figures may appear in colour only in the online journal)

1. Introduction

In less than one decade, plasmonic and metamaterial-based technologies have gained great momentum and attracted a considerable amount of human and economic resources all over the globe [1]. This is mainly due to two fundamental facts: (i) plasmonic modes can be confined well below the limit of diffraction; (ii) metamaterials allow us to arbitrarily engineer the interaction between light and matter, thus giving access to the entire optical space (ε, μ) [2, 3]. These two peculiar characteristics of plasmonics and metamaterials allowed for the experimental demonstration of nanophotonic components [4], super-resolution imaging systems [5], flat optics [6, 7], nano-lasers [8], enhanced nonlinear optics [9], metatronics [10], and many other remarkable achievements. However, despite these transformative proofs of concept, we still do not experience a widespread of nanophotonic technologies in our daily lives. This is due in great part to the

typical use of metallic inclusions in plasmonic systems that are consequently marked with high ohmic losses, lack of optical tunability and incompatibility with standard semi-conductor fabrication processes [11–13].

It is in response to all these issues that very recently the new sub-domains of all-dielectric metamaterials and nanophotonics are attracting a lot of interest. In this direction, few seminal works have experimentally proved the feasibility of nano-reso-nators [14], subwavelength meta-lenses [15], reconfigurable metamaterials [16], zero index waveguides [17], and other nano-devices without the use of metallic nano-inclusions. Other important works exploit the large nonlinearities achievable from all-dielectric systems. In this direction, it is worth mentioning the results by Shcherbakov *et al* where ultrafast reflectance mod-ulation of about 45% is attained by means of low intensity pumping using a gallium arsenide (GaAs) metasurface [18]. A similar GaAs-based structure is also used by Liu *et al* to develop an optical metamixer where, by exploiting numerous nonlinear processes, frequency generation is demonstrated for eleven new spectral lines ranging from ultraviolet to near infrared [19]. This brief overview of recent literature should give a general picture of the attention that is today paid to all-dielectric systems by many research groups all over the globe. The main advantages of high-index contrast nanodevices are ease of fabrication, high transparency and integrability. On the other hand, the require-ments on the large refractive index step ($\Delta n > 2$) drastically limits the number of possible functional materials while the resonant behavior of the dielectric inclusion reduces the max-imum operational bandwidth.

In addition, this approach does not just revolutionize the typical list of materials employed for nano-photonic appli-cations, but also changes the underlying standard analytical approach. In fact, if on the one hand metal-based nano-components are modelled with respect to the coupling between the electromagnetic radiation and the electron plasma oscillation at the metal/dielectric interface, on the other hand, all-dielectric plasmonic elements are typically modelled by using Mie scattering theory applied to high-index contrast systems [20, 21]. This corresponds to a radically new approach, which from one side addresses most of the pre-viously listed problems by eliminating metallic inclusions, but from the other side quenches the key physical mechanisms that made plasmonics so attractive in the first place.

Within this technological context, our research philoso-phy is somehow in the middle, with the ambitious goal of developing metal-free plasmonic technologies. This idea, which could sound as a contradiction in terms, has recently attracted great attention thanks to the introduction of trans-parent conducting oxides (TCOs) into the world of photonics. This class of materials will be at the center of the present work, which is not meant to be a review paper but rather an original contribution reporting novel results in the context of TCO-based tunable plasmonics. The extended introduction has the sole purpose of providing the reader with a broader view about the topic and a general knowledge of the most recent and relevant achievements. For these reasons, the list of cited articles is by no means exhaustive and the authors apologize to those who have been neglected.

1.1. Tuneable plasmonics enabled by TCOs

TCOs are a class of wide bandgap semiconductors that can withstand a very high doping level (intrinsic carrier con-centration approaching $10^{21}\,cm^{-3}$) without deterioration of their structural properties. In other words, being optically tunable, CMOS compatible and relatively transparent in a wide NIR frequency window, TCOs are a sort of 'hybrid' materials that to some extent combine the most typically desirable properties of both semiconductors and metals, thus allowing for metal-free plasmonics. A good example of such a direct elimination of metallic features in favor of TCO-based structures is reported in [22] where Kim *et al*, by simply replacing silver with gallium zinc oxide (GZO), in a previously demonstrated metasurface nano-patterning, pre-served the quarter-wave retardation functionality of the ori-ginal device with a consequent shift of the operational wavelength from the VIS to the NIR. Refocusing to the case of dynamic devices, the intrinsic large nonlinearities of TCOs have been exploited in quite few cases for the realization of tunable metamaterials. In this direction, it is useful to recall the work by Guo *et al* where they demonstrated large negative nonlinearities in the full visible window for an indium oxide (IO) nanorod array pumped in the UV [23]. The same research team, using indium tin oxide (ITO) nanorods arrays, also recorded ultra-fast optical modulation triggered by a pump in the NIR (1.5 μm) and a probe in the MIR ($\cong 2\,\mu$m) [24]. Evidence of in-plane configuration for the tunability of bulk plasmons has also been acquired by Tyborski *et al* who observed a strong redshift of the reflectivity spectra in GZO bi-layers upon intraband excitation [25]. All these key studies, and many others (not reported for the sake of brevity), unequivocally prove the feasibility of numerous energy effi-cient metal-free plasmonic devices with much reduced foot-print and great dynamic tunability. It is also worth adding that another fundamental feature of TCOs deals with the fact of having the dispersion curve of the dielectric permittivity crossing zero in within the telecom frequency range. Such a characteristic is extremely attractive for developing novel integrated photonic devices as it will be described along the next paragraph.

### 1.2. Enhanced nonlinearities in TCOs when entering the ENZ regime

As stated in the abstract of the present manuscript, TCO materials allow to access the epsilon-near-zero (ENZ) regime at telecom wavelengths in their bulk form. This is a very peculiar electromagnetic region where decoupling of spatial and temporal field variations is attained contextually with a strong wavelength 'stretching' [26]. Under these conditions many novel optical phenomena have been observed such as super-coupling [27], photonic doping [28], and largely enhanced nonlinearities [29, 30]. These giant nonlinearities can manifest themselves as an intensity dependent ultra-fast and large alteration of the complex refractive index when the material is optically pumped [31–33]. It has also been demonstrated that due to their hybrid nature, effective optical

excitation can be performed both interband and intraband with opposite effects on the material properties. Such effects can be algebraically summed up for achieving optical logic control of light or combined allowing for a considerable enlargement of the intrinsic material bandwidth [34]. All these properties, unique to TCOs, have direct application for the fabrication of optical arithmetic logic unit (ALU), efficient/compact THz detectors, ultra-fast modulators, etc. It is worth mentioning that even though all the TCOs share a general common behavior, the choice of a specific compound over another TCO can be made out of technological considerations (see supplementary information [34]). For instance, when a study wants to stress on the potential technological implications ITO is typically selected having been largely used during the last decade for the fabrication of electro-optic devices, touch screens, and photovoltaic components. Aluminum zinc oxide (AZO) and GZO instead are preferred for telecom application for their reduced losses in the NIR. More recently, other compounds such as indium cadmium oxide (ICO) have been chosen because of their superior electron mobility to enhance the efficiency of transient reflective polarizers [35]. All the works recalled so far are entirely focused on TCOs and their optical fingerprint in the ENZ frequency window in the context of all-dielectric plasmonics. However, few new studies pointed out that the combined use of metallic nano antennas with ENZ bulk materials, can reveal unexpected results. In this regard, from a static point of view, we wish to refer to the work by Kim *et al* about the role of ENZ substrates in the optical response of plasmonic antennas where highly directional re-emission and resonance 'pinning' to the ENZ wavelength are observed for gold nano-resonators deposited on AZO and GZO substrates [36]. More recently, from a dynamic point of view, the combined use of TCOs and metallic inclusion has been exploited to prove record high third order nonlinearities seven orders of magnitude larger than that of silica glass [37]. These achievements should let us keep in mind that if, from one side, it is of great interest to develop metal free nano-components, from another side, we cannot strictly limit our curiosity to a specific set of materials.

The following paragraphs will be reporting some new results dealing with the dynamic frequency tuning of optical pulses in the NIR frequency window close to the ENZ wavelength, and on how such dynamic shift is linked to both real and imaginary part of the refractive index.

2. Experiments

Figure 1 shows the set-up employed for our experiments; this was a standard pump and probe system with the pump wavelength set at 787 nm and the probe being tuneable in the range between 1150 nm and 1550 nm. The core source was a Ti:sapphire laser generating 100 fs pulses (Amplitude Technologies) with a repetition rate of 100 Hz. Such an optical pulse train was subsequently split into two parts. The one unaltered in wavelength and passing through the delay line constituted the pump signal. The second part instead was sent to an OPA for
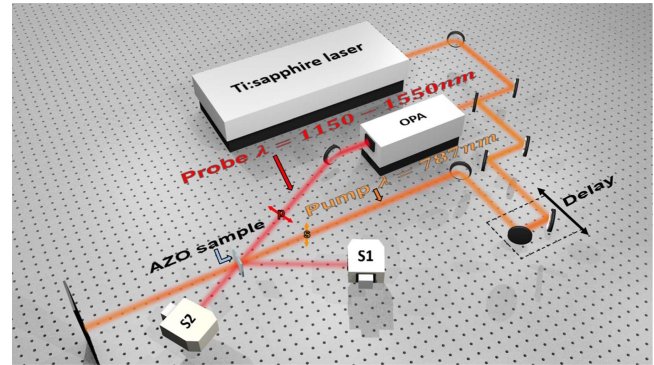

Figure 1. Experimental setup: a high intensity and p-polarized beam at 787 nm pumps a $\cong 1\,\mu m$ thin AZO film at normal incidence. The reflection and transmission of a weak probe beam (with variable wavelength between 1150 and 1550 nm, s-polarised, and an incident angle $<10°$) are simultaneously recorded.

parametric wavelength conversion into probe pulses of approximately 120 fs (Topas, Light Conversion Ltd). The probe fluence was regulated to be below the limit for triggering nonlinear effects while the intensity for the pump was brought up to $869\,\mathrm{GW\,cm^{-2}}$. In order to ensure a good spatial uniformity of the triggered refractive index change, the pump to probe surface ratio was set 7:1. Both reflected and transmitted probe spectra were recorded using ocean optics spectrometers (NIRQuest Ocean Optics) with 6 nm resolution (see S1 and S2 in figure 1). The sample consisted in a $\cong 1\,\mu m$ layer of AZO deposited on a thick 0.5 mm fused silica glass. The transparent conductive film was deposited by using pulsed laser deposition in an oxygen deprived atmosphere with the purpose to further increase the intrinsic carrier concentration and set the ENZ wavelength in the NIR around 1.3 μm [38].

3. Discussion

Figure 2 shows, in the colour bar, both the transient reflected (a) and transmitted (b) power spectral densities as a function of the time delay τ between the pump and a probe signals, with the latter set at $\lambda = 1290$ nm (few nanometres apart from the ENZ wavelength). Both plots have been corrected with respect to the power spectral density reflected at the glass/air interface. These images report a very large dynamic shift of the probe spectrum which is first red-shifted, during the excitation cycle, and then blue-shifted, along the subsequent relaxation time. The maximum absolute shift accounts for about 13 nm which is comparable to the entire probe bandwidth. These results deal with the re-distribution of hot electrons in the conduction band triggered by intraband optical excitation. Such a process can be accurately described by employing the so called two-temperature model, which accounts for both the electron and the lattice temperature and captures the material dynamic response (see supplementary information [34]).

To a first approximation, since the AZO layer is optically thin, the measured wavelength shift can be largely accounted as cross-phase modulation and roughly evaluated starting from the formula for the angular frequency shift $\Delta\omega = k_0 L \cdot (dn/dt)$,
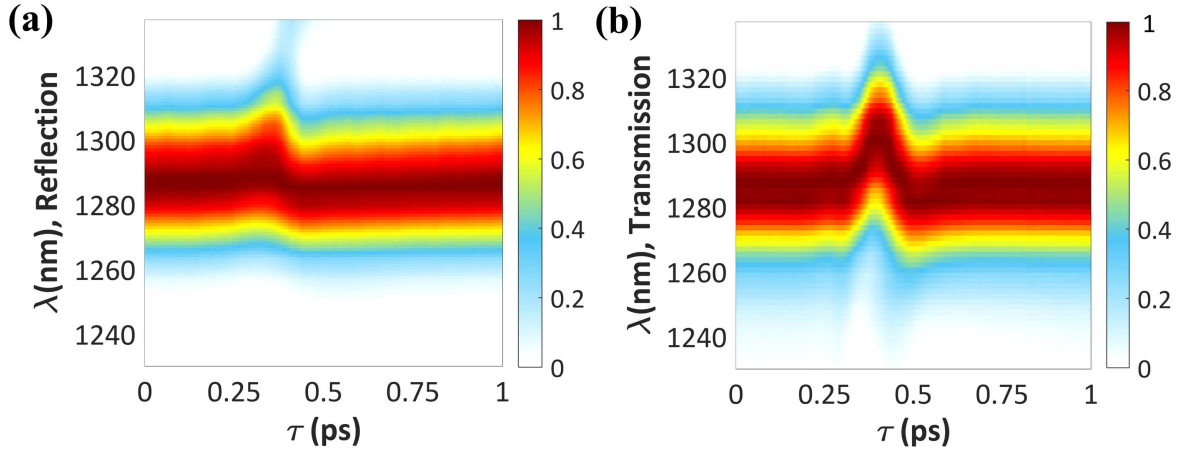
Figure 2. Transient spectrogram of the reflected (a) and transmitted (b) probe signal at 1290 nm central wavelength under NIR pump excitation of intensity $I = 869\,\mathrm{GW\,cm^{-2}}$. With τ we indicate the temporal delay between the pump and the probe signals.
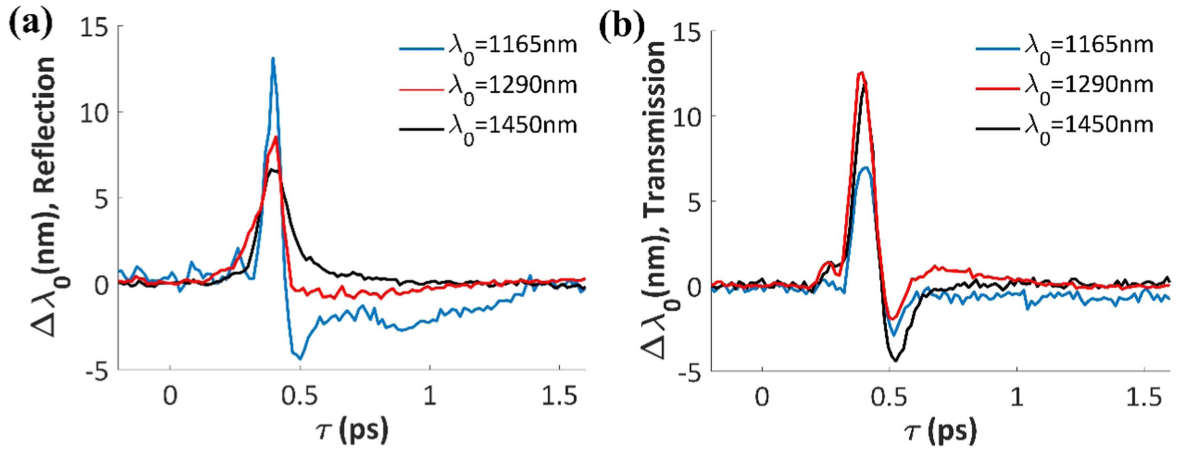
Figure 3. Carrier wavelength shift of reflected (a) and transmitted (b) probe signals at 1165 nm, 1290 nm, and 1450 nm (central wavelength) under NIR pump excitation of intensity $I = 869\,\mathrm{GW\,cm^{-2}}$.

where k_0, L, n, are the free-space wavenumber, the propagation length, and the real refractive index, respectively, and the derivative with respect to the time t is considered [38–40]. However, a more careful analysis, which takes into account both the temporal profiles of the involved optical pulses, the material losses, together with the specific time delay τ between pump and probe and their collinear propagation, reveals a non-negligible fraction of the recorded wavelength shift should be ascribed to other phenomena mostly linked to the induced variation of the imaginary part of the refractive index. Even though a more rigorous study is required to precisely describe the recorded dynamic alteration of the transmitted spectrum, the previously mentioned simplified model can already grasp the curve shapes reported in figure 2 just starting from the temporal dynamics of the complex refractive index [34]. Even if the employed pump fluence is relatively large (tens of mJ/cm²), the magnitude and speed of the induced frequency shift let us believe that our attainments could be of interest for those applications where the need for ultra-high operational speed prevails over energy consumption considerations.

It is worth underlying that the recorded spectral shift $\Delta\lambda_0$ is strongly wavelength dependent as it is apparent from the graphs in figures 3(a) and (b). Here the central wavelength detuning of the reflected (a) and transmitted (b) probe are plotted as a function of τ for three different values of the probe wavelength. As we can see, in reflection the maximum absolute value of $\Delta\lambda_0$ monotonically increases for decreasing values of the probe wavelength reaching a peak of about 13 nm at $\lambda_0 = 1165\,\mathrm{nm}$. In transmission, because of energy conservation, we expect the opposite trend, however this is strictly true only if we neglect the induced changes in the material absorption (i.e. variation of the imaginary refractive index). From figure 3(b), the maximum absolute shift in transmission increases with the wavelength and saturates at $\lambda_0 = 1290\,\mathrm{nm}$ (close to the ENZ wavelength $\lambda_{ENZ} = 1300\,\mathrm{nm}$) to a maximum value of about 12 nm. For the transmitted signal, optimal modulation occurs when the quantity $\Delta n_r / \alpha$ (where n_r is the real part of the refractive index and α is the material linear absorption) is maximized. In fact, the maximum variation of the real part of the refractive index is observed at the ENZ

wavelength, whereas the linear absorption decreases at longer wavelengths [31].

It is important noticing that by changing the temporal distance τ it is possible to induce either a red- or a blue-shift in the probe spectrum. If we consider the entire temporal dynamics, an overall wavelength shift of about 17 nm is attainable for both the reflected and the transmitted signals, a value which is comparable with the entire pulse bandwidth. However, if the described tuning capabilities are to be used for practical implementation of optical signal routing, only the maximum $\Delta\lambda_0$ at a given τ should be considered. In this case, the suitable wavelength shift is equivalent to the bandwidth of a transform limited pulse with a time duration of 200 fs.

The study of the wavelength detuning as a function of the probe central wavelength, which is reported here, is complementary to the investigation of the wavelength shift as a function of the pump intensity I reported in [31], where a linear trend is recorded for $\Delta\lambda_0$ Vs I. Although the ultra-fast spectral modulation of optical signals mediated by non-linearities in TCOs has already been presented to some extent in previous works [31–34], here for the first time we show the transient behavior of the entire pulse spectrum in both reflection and transmission, as well as a study of the shift as a function of the probe wavelength. These are all key information for designing integrated optical routers and switches operating at telecommunication wavelengths. Furthermore, these results plus those already published, demonstrate an unprecedented flexibility in controlling the optical properties of TCOs. These compounds provide many options for the static tunability of their optical properties, which can be attained by changing either their stoichiometry or the growth parameters. In addition to these degrees of freedom, our results also prove the unique capability of TCOs to arbitrary engineer their ultra-fast and large induced change of the complex refractive index by simply changing the operational wavelength and/or the pumping mode (i.e. either interband or intraband).

4. Conclusions

In conclusion, we have discussed many fundamental reasons making TCO-based technology extremely appealing for the development of new ultra-fast nano-photonics devices. Among these reasons, we find the need for low-loss components which are also tunable and CMOS compatible. A short overview of the most relevant and recent achievements in the emerging field of metal-free plasmonics have been provided with particular attention to photonic devices employing TCOs as core materials. Additionally, the added advantage of having access to the ENZ regime for bulk materials, and in the full telecom window, has also been elucidated by giving few remarkable examples. Along the line of enhanced non-linearities in ENZ materials we have also presented few results dealing with the ultra-fast routing of optical signals. Our attainments demonstrate carrier frequency shifts, attained via intraband optical excitation, which are equivalent to the

bandwidth of a transform limited Gaussian pulse of 200 fs. Such dynamic optical tuning can be engineered by a relatively small change in either the probe wavelength or in the excitation process (i.e. interband or intraband). The recently published literature on TCOs, plus the results reported in the present manuscript, define this class of materials as one of the most promising for future tunable nano-photonic components.

ORCID iDs

Marcello Ferrera ⓘ https://orcid.org/0000-0003-4479-5127

References

[1] Pelton M and Bryant G 2013 *Introduction to Metal—Nanoparticle Plasmonics* (Hoboken, NJ: Wiley)

[2] Cai W and Shalaev V M 2010 *Optical Metamaterials: Fundamentals and Applications* (New York: Springer)

[3] Bozhevolnyi S 2009 *Plasmonic Nanoguides and Circuits* (Singapore: Pan Stanford)

[4] Haffner C *et al* 2015 All-plasmonic Mach–Zehnder modulator enabling optical high-speed communication at the microscale *Nat. Photonics* **9** 525–8

[5] Lu D and Liu Z 2012 Hyperlenses and metalenses for far-field super-resolution imaging *Nat. Commun.* **5** 1205

[6] Yu N, Genevet P, Kats M A, Aieta F, Tetienne J P, Capasso F and Gaburro Z 2011 Light propagation with phase discontinuities: generalized laws of reflection and refraction *Science* **334** 333–7

[7] Kildishev A V, Boltasseva A and Shalaev V M 2013 Planar photonics with metasurfaces *Science* **339** 123200

[8] Stockman M 2014 Plasmonic lasers: on the fast track *Nat. Phys.* **10** 799–800

[9] Kauranen M and Zayats A V 2012 Nonlinear plasmonics *Nat. Photonics* **6** 737–48

[10] Li Y, Liberal I, Della Giovampaola C and Engheta N 2016 Waveguide metatronics: lumped circuitry based on structural dispersion *Sci. Adv.* **2** e1501790

[11] Khurgin J B 2015 How to deal with the loss in plasmonics and metamaterials *Nat. Nanotechnol.* **10** 2–6

[12] Ferrera M, Kinsey N, Shaltout A, Devault C, Shalaev V and Boltasseva A 2016 Dynamic nanophotonics *J. Opt. Soc. Am. B* **34** 95–103

[13] Naik G V, Shalaev V M and Boltasseva A 2013 Alternative plasmonic materials: beyond gold and silver *Adv. Mater.* **25** 3264–94

[14] Yang Y, Miller O D, Christensen T, Joannopoulos J D and Soljačić M 2017 Low-loss plasmonic dielectric nanoresonators *Nano Lett.* **17** 3238–45

[15] Fan W, Yan B, Wang Z and Wu L 2016 Three-dimensional all-dielectric metamaterial solid immersion lens for subwavelength imaging at visible frequencies *Sci. Adv.* **2** e1600901

[16] Karvounis A, Ou J Y, Wu W, MacDonald K F and Zheludev N Y 2015 Nano-optomechanical nonlinear dielectric metamaterials *Appl. Phys. Lett.* **107** 191110

[17] Li Y, Kita S, Muñoz P, Reshef O, Vulis D I, Yin M, Lončar M and Mazur E 2015 On-chip zero-index metamaterials *Nat. Photonics* **9** 738–42

[18] Shcherbakov M R *et al* 2017 Ultrafast all-optical tuning of direct-gap semiconductor metasurfaces *Nat. Commun.* **8** 17

[19] Liu S, Vabishchevich P P, Vaskin A, Reno J L, Keeler G A, Sinclair M B, Staude I and Brener I 2017 An optical metamixer arXiv:1711.00090

[20] Jahani S and Jacob Z 2016 All-dielectric metamaterials *Nat. Nanotechnol.* **11** 23–36

[21] Devilez A, Zambrana-Puyalto Z, Stout B and Bonod N 2015 Mimicking localized surface plasmons with dielectric particles *Phys. Rev.* B **92** 241412

[22] Kim J, Choudhury S, DeVault C, Zhao Y, Kildishev A V, Shalaev V M, Alù A and Boltasseva A 2016 Controlling the polarization state of light with plasmonic metal oxide metasurface *ACS Nano* **10** 9326–33

[23] Guo P, Chang R P H and Schaller R D 2017 Transient negative optical nonlinearity of indium oxide nanorods arrays in the full-visible range *ACS Photonics* **4** 1494–500

[24] Guo P, Schaller R D, Ketterson J B and Chang R P H 2016 Ultrafast switching of tunable infrared plasmons in indium tin oxide nanorod arrays with large absolute amplitude *Nat. Photonics* **10** 267–73

[25] Tyborski T, Kalusniak S, Sadofev S, Henneberger F, Woerner M and Elsaesser T 2015 Ultrafast nonlinear response of bulk plasmons in highly doped ZnO layers *Phys. Rev. Lett.* **115** 147401

[26] Liberal I and Engheta N 2017 Near-zero refractive index photonics *Nat. Photonics* **11** 149–58

[27] Edwards B, Alù A, Young M E, Silveirinha M and Engheta N 2008 Experimental verification of epsilon-near-zero metamaterial coupling and energy squeezing using a microwave waveguide *Phys. Rev. Lett.* **100** 033903

[28] Liberal I and Engheta N 2017 Photonic doping of epsilon-near-zero media *Science* **355** 1058–62

[29] Kinsey N, DeVault C, Kim J, Ferrera M, Shalaev V M and Boltasseva A 2015 Epsilon-near-zero Al-doped ZnO for ultrafast switching at telecom wavelengths *Optica* **2** 616–22

[30] Traviss D, Bruck R, Mills B, Abb M and Muskens O L 2013 Ultrafast plasmonics using transparent conductive oxide hybrids in the epsilon-near-zero regime *Appl. Phys. Lett.* **102** 121112

[31] Caspani L *et al* 2016 Enhanced nonlinear refractive index in ε-near-zero materials *Phys. Rev. Lett.* **116** 233901

[32] Alam M Z, De Leon I and Boyd R W 2016 Large optical nonlinearity of indium tin oxide in its epsilon-near-zero region *Science* **352** 795–7

[33] Reshef O, Giese E, Alam M Z, De Leon I, Upham J and Boyd R W 2017 Beyond the perturbative description of the nonlinear optical response of low-index materials *Opt. Lett.* **42** 3225–8

[34] Clerici M *et al* 2017 Controlling hybrid nonlinearities in transparent conducting oxides via two-colour excitation *Nat. Commun.* **8** 15829

[35] Yang Y, Kelley K, Sachet E, Campione S, Luk T S, Maria J P, Sinclair M B and Brener I 2017 Femtosecond optical polarization switching using a cadmium oxide-based perfect absorber *Nat. Photonics* **11** 390–5

[36] Kim J *et al* 2016 Role of epsilon-near-zero substrates in the optical response of plasmonic antennas *Optica* **3** 339–46

[37] Alam M Z, Schulz S A, Upham J, D Leon I and Boyd R W 2017 Unity-order nonlinear index change in a metasurface *Proc. Photonics North 2017 (Ottawa, 6–8 June 2017)* 255-wx55-265

[38] Urbas A M *et al* 2016 Roadmap on optical metamaterials *J. Opt.* **18** 093005

[39] Mehta P, Healy N, Day T D, Badding J V and Peacock A C 2012 Ultrafast wavelength conversion via cross-phase modulation in hydrogenated amorphous silicon optical fibers *Opt. Express* **20** 26110–6

[40] Shaltout A, Clerici M, Kinsey N, Kaipurath R, Kim J, Carnemolla E, Faccio D, Boltasseva A, Shalaev V M and Ferrera M 2016 Doppler-shift emulation using highly time-refracting TCO layer *Conf. on Lasers and Electro-Optics, OSA Technical Digest (online)* (Optical Society of America) 2016FF2D.6